TECHNISCHE UNIVERSITÄT WIEN

D I P L O M A R B E I T

Chemical and physical impact on the Szilárd-Chalmers-effect: using the example of molybdenum

Ausgeführt am Institut für

Angewandte Synthesechemie

und am

Atominstitut

der Technischen Universität Wien

unter der Anleitung von

Privatdoz. Dipl.-Ing. Dr.techn. Peter Weinberger

und

Univ.-Prof. Mag.rer.nat. Dr.techn. Georg Steinhauser

und

Univ.Ass. Dr.rer.nat. Jan Matthew Welch

als verantwortlich mitwirkenden Universitätsassistenten

durch

Veronika Rosecker

Josef-Weinhebergasse 4/1/8, 2340 Mödling

Wien, am 15.03.2017 Veronika Rosecker

Abstract

Szilárd-Chalmers reactions are a potential alternative route to the production of medically important ^{99}Mo. In this work, four substituted molybdenum(IV) oxophthalocyanines were synthesised, irradiated and analysed regarding syntheses and purification, thermal stability, radiochemical yield of ^{99}Mo in the target material and substitution effects on the retention.

Molybdenum(IV) oxophthalocyanines were synthesized from substituted (-F, -NO_2, -CH_3) 1,2-dicyanobenzenes with ammonium heptamolybdate tetrahydrate in a melt at ~170 °C. Purification by sublimation at 450 °C and 0.06 mbar was successful for the unsubstituted material and gave a dark blue powder. The compounds were characterized by IR, UV/VIS and powder diffraction. The Mo=O vibration in IR spectra of the unsubstituted Molybdenum(IV) oxophthalocyanine (965 cm^{-1}) and the calculated vibration at 994 cm^{-1} show good agreement and indicates the desired oxidation state of +IV for molybdenum - the absence of the Mo≡N vibration at 1078 cm^{-1} confirms this. Irradiation experiments were carried out in dry irradiation tubes at the edge of the core (neutron flux: $2 \cdot 10^{12}$ $cm^{-2}s^{-1}$) of the TRIGA mark II research reactor at the TU Wien.

The highest radiochemical yields were obtained with the unsubstituted Molybdenum(IV) oxophthalocyanine, whereas the highest yields of carrier-free ^{99}Mo after separation were obtained with the NO_2 and CH_3 substituted phthalocyanines (>90 %). Using a Linear Free Energy Relationships (LFER; Hammett-equation) substitution effects during irradiation were investigated. No substituent effect were observed in the radiochemical yields, whereas an influence on the retention seems likely. It seems that the recombination reaction resulting in retention of the activated nucleus involves a positive charge, but further experiments are required.

From the results obtained in this work the methyl-substituted molybdenum(IV) oxophthalocyanine is the most promising candidate regarding synthesis, purification, irradiation and retention for further investigations.

Deutsche Kurzfassung

Szilárd-Chalmers Reaktionen sind ein möglicher alternativer Weg zur Produktion des medizinisch wichtigen Radioisotops ^{99}Mo. In dieser Arbeit wurden vier substituierte Molybdän(IV)oxophthalocyanine synthetisiert und mit Neutronen bestrahlt. Neben Aufreinigung, Charakterisierung und thermischer Analyse der Substanzen wurde auch die radiochemische Ausbeute an ^{99}Mo sowie der Einfluss der Substituenten auf die Retention untersucht.

Molybdän(IV)oxophthalocyanine wurden aus substituierten (-F, -NO_2, -CH_3) 1,2-Dicyanobenzol mit Ammoniumheptamolybdat-tetrahydrat bei ~170 °C in der Schmelze synthetisiert. Die Aufreinigung über Sublimation im Vakuum bei 450 °C und 0.06 mbar war für das unsubstituierte Molekül erfolgreich und ergab ein dunkelblaues Pulver. Alle synthetisierten Verbindungen wurden mittels IR, UV/VIS und Pulverdiffraktometrie charakterisiert. Die gemessene Mo=O Schwingung des unsubstituierten Molybdän(IV)oxophthalocyanins im IR (965 cm^{-1}) und die berechnete Schwingung (994 cm^{-1}) zeigen eine gute Übereinstimmung und weisen auf die erwartete Oxidationsstufe von +IV des Molybdäns hin. Die Abwesenheit der Mo≡N Schwingung bei 1078 cm^{-1} bestätigt dies. Die Bestrahlungsexperimente wurden in Trockenbestrahlungsrohren am Rande des Reaktorkerns (Neutronenfluss: $2 \cdot 10^{12}$ $cm^{-2}s^{-1}$) des TRIGA Mark II Forschungsreaktors an der TU Wien durchgeführt.

Die höchsten radiochemischen Ausbeuten wurden mit dem unsubstituierten Molybdän(IV)oxophthalocyanin erzielt, die höchsten Ausbeuten an trägerfreien ^{99}Mo nach der Abtrennung konnten mit den NO_2 und CH_3 substituierten Verbindungen erreicht werden (> 90 %). Mögliche Substituenteneffekte wurden mittels Linear Free Energy Relationships (LFER; Hammett-Gleichung) untersucht. Es konnte kein Einfluss der Substituenten auf die radiochemische Ausbeute festgestellt werden, allerdings dürften Substituenteneffekte bei der Retention eine Rolle spielen. Möglicherweise verlaufen Rekombinationsreaktionen über eine positiv geladene Zwischenstufe – um eine gesicherte Aussage zu machen sind weitere Experimente notwendig.

Von allen synthetisierten Verbindungen scheint das CH_3 substituierte Molybdän(IV)oxophthalocyanin der vielversprechendste Kandidat bezüglich Synthese, Aufreinigung, Bestrahlung und Retention für weitere Untersuchungen zu sein.

Danksagung

Zuerst möchte ich mich bei meinen Betreuern, insbesondere Prof. Peter Weinberger bedanken, der die Betreuung meiner Arbeit übernahm, obwohl sie thematisch doch etwas abseits seines Forschungsbereichs liegt.

Mein besonderer Dank gilt Dr. Jan Welch, welcher mir nicht nur den einen oder anderen Trick im Labor zeigte, sondern auch jederzeit für meine (oft mehrfach gestellten) Fragen zur Verfügung stand und nicht zuletzt für die unzähligen Diskussionen, Anregungen und Korrekturen die dieser Arbeit vorangegangen sind.

Herzlich bedanken möchte ich mich bei Dr. Johannes Sterba, der nicht nur sein Labor zur Verfügung gestellt hat, sondern mich überhaupt ans Atominstitut gebracht hat. Ein großes Dankeschön auch an Michaela Foster für ihre unermüdliche Unterstützung und Hilfe bei der täglichen Arbeit im Labor – jemand Besseren kann man sich nicht wünschen.

Ebenso möchte ich mich auch bei der Arbeitsgruppe von Prof. Peter Weinberger für ihre Unterstützung bedanken, insbesondere bei DI Christian Knoll für seine rasche und unkomplizierte Hilfe bei täglichen Problemen der Chemie, aber vor allem bei der Charakterisierung meiner Verbindungen. Die theoretischen Berechnungen wurden am Vienna Scientific Cluster 3 (VSC-3) durchgeführt.

Nicht zu vergessen sind die Mitarbeiter der Reaktorcrew, insbesondere Dr. Mario Villa und DI Robert Bergmann sowie dem Team des Strahlenschutzes am Atominstitut die immer mit Rat und Tat zur Seite stehen und ohne die ich die Bestrahlungsexperimente nicht durchführen hätte können.

Zu guter Letzt möchte ich mich auch bei Prof. Thorsten Schumm bedanken. Einerseits für die Möglichkeit in seiner Gruppe zu arbeiten und der dadurch entstandenen finanziellen Unterstützung und andererseits für sein Verständnis, wenn ich manchmal doch mehr an Molybdän als an Thorium gearbeitet habe.

Table of contents

1 Introduction

Ionizing radiation and radionuclides have found application in medicine since their respective discoveries. For example, Wilhelm Conrad Roentgen discovered X-rays in 1895 and X-ray imaging rapidly became a standard diagnostic technique. With the isolation of macroscopic amounts of radium in 1902 and the description of its anti-tumor properties, the application of radioisotopes in medicine started to become a topic of interest. In modern nuclear medicine, X-rays are used almost exclusively for diagnosis and imaging and particle radiation from accelerators is used predominantly for therapy, radioisotopes can be used for both – diagnosis and therapy.

1.1 Modern Nuclear Medicine

Nuclear medicine may be defined as application of ionizing radiation to the body, either for therapy or imaging. More explicitly, in radiotherapy sealed radioactive substances are used, which cannot interact with their environment. In nuclear medicine unsealed radioactive substances are applied which interact with their environment, for example biochemically (Figure 1). Unsealed radioactive sources are typically incorporated as a drug in which the radioactive isotope is chemically bound to the drug (radiopharmaceutical). Radiopharmaceuticals may be used for both, radiotherapy (α- or β^--emitter) and radioimaging (β^+- or γ-emitter). By exchanging an atom in a drug molecule with a radioisotope the chemical and biological properties are not significantly changed and, therefore, the behaviour in biological environment (e.g. distribution, metabolism) will be the same as in an unlabelled molecule. Labelled molecules can thus be utilized to assess distribution and concentration by measuring the radiation with an external detector.

Radiotherapy may be divided into three main categories: teletherapy, brachytherapy and therapy with unsealed sources (radionuclide therapy). In teletherapy sealed radiation sources or particle accelerators are used for treatment from outside the body. Whereas in brachytherapy internally applied sealed radioactive sources may be inserted as a small capsule into a tumor or next to it to obtain the highest possible radiation dose. Radionuclide therapy uses radiopharmaceuticals which are mainly accumulated in the organ where the radioisotope deposits its energy directly into or next to the target.

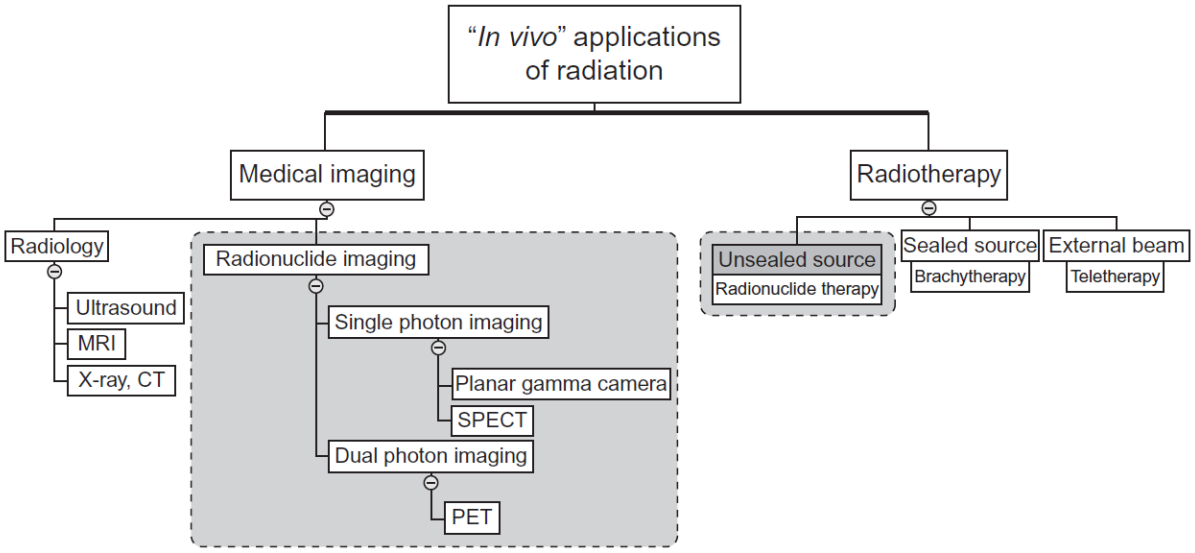

Figure 1: Overview of use of radiation in medicine [1] *– grey: fields of nuclear medicine*

In conventional imaging techniques, such as X-rays, ultrasound and magnetic resonance structural information about the tissue is obtained. Whereas radionuclide imaging utilizes gamma cameras (scinitigraphy), Single Photon Emission Computer Tomography (SPECT) and Positron Emission Tomography (PET) to examine the function of tissues and organs since metabolism can be monitored. SPECT and PET are both tomography methods which require the detectors to move around the patient to obtain images layer by layer which can be combined into a 3D image by post-processing. PET requires positron emitters, whereas SPECT may utilize the same radionuclides as for gamma cameras. For scintigraphy static gamma cameras are used and 2D images are obtained. Several images may be acquired per minute, so time-dependent imaging is also possible. The most widespread radionuclide imaging technique is scintigraphy (~95 %) as it is broad applicable and a comparative fast and simple radioimaging technique.[2]

The gamma radiation needed for nuclear imaging (for PET, the emitted positron is annihilated to two gamma photons) is always a by-product of some other nuclear decay. As α- and β^--emitters would expose the patient to unnecessary additional radiation, pure gamma emitters are required. There are two types of decay that yield pure gamma emission: electron capture and metastable isotopes (nuclear isomers). A metastable state may occur after β-decay in which the daughter nuclei remain in an excited state. Relaxation to the ground state releases energy as a gamma photon. Additionally, the half-life of the radioisotope should be in a range of a few hours to minimize patient radiation exposure. Because of its unique properties the most commonly gamma emitter used for radioimaging is ^{99m}Tc. ^{99m}Tc is distinguished by its moderate half-life of 6 h and gamma energy of 140 keV.[1]

2 State of the Art

2.1 ^{99m}Tc usage

Due to its unique properties, ^{99m}Tc is the work horse in nuclear medicine. The gamma energy of 140 keV makes the isotope perfect for routine use, because with this energy common sodium iodide gamma detectors can be used without further modification. ^{99m}Tc can be used in several different ways for a large variety of medical indications: pertechnate $^{99m}TcO_4^-$ (renal imaging), phosphate (bone), chelated (kidney, bladder, spleen and colon), sulphur colloid (kidney) or microaggregated albumin (lung, liver, spleen and kidney). Also some ^{99m}Tc aerosols have been developed for lung scans. Depending on chemical environment it can also pass the blood-brain-barrier, so brain imaging is also possible.[3]

2.2 From ^{99}Mo to ^{99m}Tc

^{99}Mo is a β^- emitting artificial radioisotope of molybdenum that decays to ^{99m}Tc with a half-life of 66 h. ^{99m}Tc is the metastable state of the radioisotope ^{99}Tc. ^{99m}Tc decays into ^{99}Tc with a half-life of 6 h and emits thereby a gamma photon with an energy of 140 keV (see Figure 2). ^{99}Tc itself is also a β^--emitter with a half-life over $2 \cdot 10^5$ years, thus the specific activity is very low and can be neglected with respect to biological half-life.

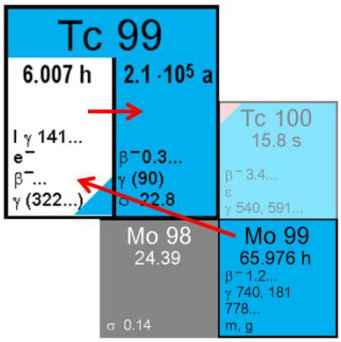

Figure 2: Excerpt from the Karlsruhe Nuclide Chart, 2012

2.3 Manufacturing chain of ^{99}Mo

The production of ^{99}Mo for use can be separated in several steps: Production of targets, irradiation, chemical processing, generator production and packaging. When produced via fission, targets are made out of uranium-aluminium alloys, uranium oxide or uranium metal enriched in ^{235}U. Irradiation of the targets is performed in a few high-flux research reactors worldwide. After irradiation, the targets are chemically processed to separate the ^{99}Mo from other fission products. The pure ^{99}Mo is then adsorbed on alumina columns and packed into shielded generators. These generators are then shipped to hospitals where ^{99m}Tc, the daughter product of ^{99}Mo, can be easily extracted with ammonia or physiological sodium chloride solution for diagnostic use.

2.3.1 Production methods for ^{99}Mo

There are two main production methods for medical ^{99}Mo: the fission of ^{235}U and the neutron capture by ^{98}Mo. Both methods have advantages and disadvantages. For medical purposes a high specific activity (activity [Bq or Ci] per volume or mass) of ^{99}Mo is required to gain high yields and pure ^{99m}Tc. Also radioactive waste production should be minimal. The two approaches are compared in Table 1.

Table 1: Comparison of ^{99}Mo produced from fission and neutron capture [3]

^{235}U(n,f)^{99}Mo	^{98}Mo(n,γ)^{99}Mo
Produces high specific activity ^{99}Mo	Produces low specific activity ^{99}Mo
Requires enriched ^{235}U target	Requires highly enriched ^{98}Mo target
Complex chemical processing	Simple chemical processing
Requires dedicated processing facility	Requires high flux neutron source
Generates high-level radioactive waste	Generates minimal waste

2.3.1.1 Fission produced ^{99}Mo [3]

The fission of ^{235}U by thermal neutrons produces a great variety of radioisotopes, including about 6 % ^{99}Mo (Figure 3). The amount of ^{99}Mo produced depends on several conditions including the degree of enrichment of ^{235}U E, the neutron flux θ, precise neutron energy, and the cross section σ of the nuclear reaction (see Equation 1).

Equation 1

$$n(^{99}Mo) \propto E(^{235}U)\,\theta\,\sigma$$

The cross section for fission of ^{235}U is quite large (about 600 barns; 1 barn = 10^{-24} cm^2). About 6 % of the thermal fission products will produce ^{99}Mo – equates to an effective cross section about 36 barns. In an average reactor, an irradiation time of five to seven days is necessary to obtain an optimal amount of ^{99}Mo.[3]

As only 6 % of the fission products are ^{99}Mo, a large amount of radioactive waste material is concomitantly produced. Some of the other fission products including ^{131}I and ^{133}Xe can also be used for medical purposes but most of the fission material that remains is highly radioactive waste and has to be specially treated and stored.

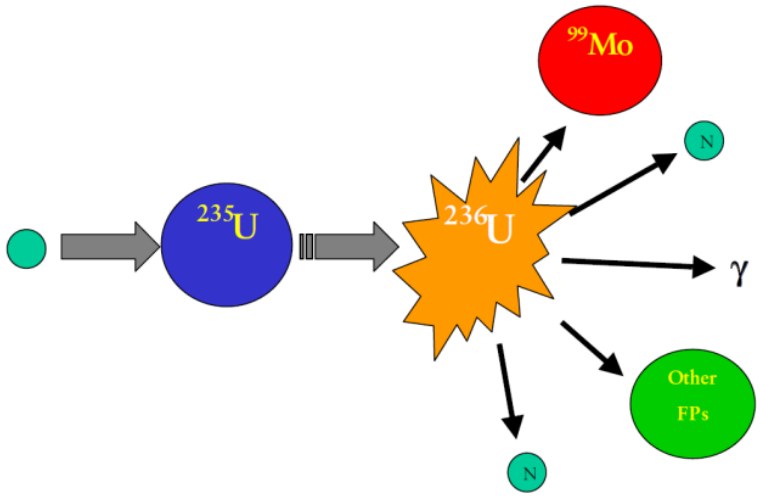

Figure 3: Fission produced ^{99}Mo (schematic); N...neutron, FPs...fission products [3]

As natural uranium contains only 0.72 % ^{235}U it must be enriched to be useful as target material and/or fuel in light-water moderated nuclear reactors. There are two types of targets/fuels: highly enriched uranium (HEU) and low enriched uranium (LEU). In LEU targets ^{235}U is enriched to < 20 %, HEU targets contain 20 % or more ^{235}U. Regarding nuclear safety, the International Atomic Energy Agency (IAEA) has stipulated that fuel material should be LEU in order to minimize the risks of nuclear weapon proliferation. LEU targets for ^{99}Mo production require higher neutron fluxes to compensate the smaller amount of ^{235}U in the targets but they are safer than HEU targets since the enrichment is not high enough for direct use in nuclear weapons.

But there are also some neglected aspects in the use of LEU targets. As LEU targets contain maximally 20 % ^{235}U the remaining ≥80 % uranium is ^{238}U. Reaction of ^{238}U with thermal neutrons leads to ^{239}Np ($t_{1/2}$ = 2.4 d) which decays to ^{239}Pu, which may also be used for nuclear weapons. Irradiation time (a few days), neutron flux and work-up are quite similar for the production of ^{99}Mo and ^{239}Pu. Longer irradiation time would not be that concerning, as ^{239}Pu, in part would react to ^{240}Pu which itself cannot be used for nuclear weapons. [4,5]

Beside proliferation problems there are also waste issues. With a fission yield between 5-6 % ^{90}Sr ($t_{1/2}$ = 28.9 a) and ^{137}Cs ($t_{1/2}$ = 30.1 a) are also produced for every ^{99}Mo nuclei independent of the use of HEU or LEU. Production of ^{99}Mo by fission of HEU targets also contribute significantly to the radioxenon background of the world. Attempts to verify the Comprehensive Nuclear-Test-Ban Treaty are greatly affected by this background.[6]

2.3.1.2 Neutron capture produced ^{99}Mo

In nature molybdenum exists as a mixture of seven different isotopes: 92, 14.53 %; 94, 9.15 %; 95, 15.84 %; 96, 16.67 %; 97, 9.60 %; 98, 24.38 %; 100, 9.82 %. Bombarding a ^{98}Mo nucleus with thermal neutrons causes the ^{98}Mo nuclei to absorb a neutron and become a new isotope: ^{99}Mo (^{98}Mo(n,γ)^{99}Mo) (see Figure 4).

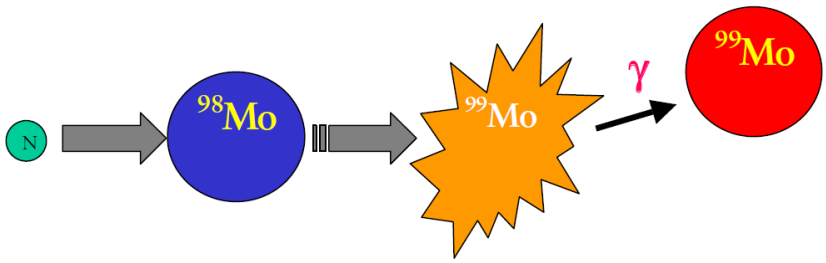

Figure 4: Neutron capture produced ^{99}Mo (schematic); N...neutron [3]

The cross section for this reaction is 0.14 barn for ^{98}Mo and effectively only 0.03 barn for natural molybdenum. In comparison, the cross section for fission produced ^{99}Mo is about 36 barns – 1200 times higher. For compensation, enriched ^{98}Mo samples or large quantities of target material must be used. Also a high neutron flux helps to compensate for the small neutron cross section (see Equation 1).

2.3.2 Processing the ^{99}Mo

The irradiated targets are processed in external processing facilities. Currently four facilities worldwide produce medical grade ^{99}Mo: Medical Device Supply (MDS) Nordion in Canada, Institute for radioelements (IRE) in Belgium, Covidien in the Netherlands and NTP in South Africa. There the target must be processed quickly to minimize the loss of ^{99}Mo from radioactive decay. Two processes are described: alkaline dissolution and acidic dissolution – both can be used for either HEU or LEU targets.

2.3.2.1 Alkaline Dissolution[3]

In the alkaline processes the whole target (including the aluminium cladding) is dissolved in sodium hydroxide solution. As the uranium in the target is uranium-aluminium alloy, the products of the dissolution are sodium aluminate and sodium molybdate. The solid residue contains most of the fission products except gases and alkali metals. The molybdenum containing solution is purified by several ion exchange steps: anion exchange resin, acryl ester resin to separate free metal ions, cation exchange and anion exchange resin. After the last separation step the ^{99}Mo is sublimed as K_2MoO_4 for further purification.[7] The purified ^{99}Mo is then adsorbed on alumina and placed in a ^{99}Mo/^{99m}Tc generator. From the alumina column the decay product ^{99m}Tc can easily be eluted in high radiochemical purity with physiological sodium chloride solution.

2.3.2.2 Acidic Dissolution[3]

Acidic dissolution is used with uranium metal or uranium oxide targets. As only the target is processed first the cladding is removed mechanically. The separated targets are then dissolved in nitric acid and all fission products except gases are dissolved as nitrates. The purification of the ^{99}Mo requires several steps of ion exchange and solvent extraction similar to the alkaline dissolution process. The final step is the same as in the alkaline process.

In both of the dissolution processes a large amount of radioactive waste – solid and liquid – accumulates. Also, most of the uranium originally in the targets ends up as radioactive waste. So in the waste of the ^{99}Mo production is a large amount of HEU is still present. Efforts to recycle this HEU are not made currently[3].

2.4 ^{99}Mo crisis

The majority of the ^{99}Mo is produced in only five reactors worldwide: Chalk River in Canada 40 %, BR-2 in Belgium 30 %, HFR Petten in the Netherlands 10-15 %, Safari-1 in South Africa 10-15 % and Osiris in France 5-8 %. All of these reactors are over 40 years old and all use HEU targets. They were not initially built for radioisotope production and produce ^{99}Mo as a revenue-generating service.

As all of the reactors discussed above are quite old, they require consistent maintenance. Since 2008, several unplanned shut downs occurred due to leakages and other aging related problems. So, in addition to planned off-line time, several unplanned operational interruptions occurred. This caused a serious shortage in the ^{99}Mo supply worldwide forcing medical professionals to use inferior alternative or older imaging methods.

Since then several small research reactors have joined the ^{99}Mo market, mainly to provide local medical isotope supplies: RA-3 in Argentina, OPAL in Australia, MARIA in Poland, GA SIWABESSY MPR in Indonesia and WWR-TS and IRT-T in Russia. Ra-3 in Argentina and OPAL in Australia are the only two reactors using LEU for the ^{99}Mo production. Australia and Poland also plan to enter the global market.

2.5 Other production methods

With the so called molybdenum crisis, alternative production methods have become of interest in research and development.

2.5.1 Medical isotope production system (MIPS)

The idea of an MIPS is a nuclear reactor with liquid fuel. In the cylindrical reactor vessel are control rods and cooling installations surrounded with a neutron reflector. The liquid fuel is an LEU salt, dissolved in nitric acid. This reactor should work in batch mode: first the ^{99}Mo concentration is build up through fission of ^{235}U and then the whole fuel solution with the ^{99}Mo and other fission products are adsorbed onto an ion exchange column. The ^{99}Mo can thus be recovered. The remaining fuel solution can be separated from other fission products and be reused.

2.5.2 Accelerator-based ^{99}Mo production[3]

There are several approaches for the accelerator-based production of ^{99}Mo. The first uses spallation neutrons from an accelerator to produce ^{99}Mo in the same way as in the fission produced ^{99}Mo. The main challenge in this approach will be the production of neutron fluxes large enough to produce comparable amounts of ^{99}Mo to a reactor.

A second approach uses the ^{100}Mo(γ,n)^{99}Mo reaction. In an accelerator, an electron beam would be used to generate high energy photons which would collide with enriched ^{100}Mo to react to ^{99}Mo. In this approach there are similar problems to those described before. In addition, the technical challenge of producing and handling beam-flux comparable with fission produced ^{99}Mo is also significant. Finally, ^{100}Mo (natural abundance: 9.82 %; half-life: $7 \cdot 10^{18}$ a) can only be used when enriched.

Yet, another potential approach is the photo-fission of ^{238}U. As ^{238}U is the main isotope (natural abundance: 99.3 %) of uranium there is no need for prior enrichment and the fission yield of ^{238}U is nearly the same as it is in ^{235}U – about 6 %. But there is the same problem as with the $^{100}Mo(\gamma,n)^{99}Mo$ reaction to obtain high enough beam fluxes to compensate the smaller cross section for the fission of ^{238}U compared to ^{235}U (approximately three orders of magnitude). The fission yield also depends on the energy of the electrons: energies above 30 MeV would be optimal, below 10 MeV there is almost no fission.[8,9]

2.5.3 Direct production of ^{99m}Tc[3]

There have been attempts to produce ^{99m}Tc directly via the $^{100}Mo(p,2n)^{99m}Tc$ reaction in an accelerator. Beside technical challenges, there is also the disadvantage of the short half-life of ^{99m}Tc with 6 h. Thus, production facilities have to be geographically proximate to hospitals and, therefore, decentralized. Shipping over large distances would require much higher activities or would not be feasible.

2.6 Szilárd-Chalmers-Reactions

Szilárd-Chalmers (S-C) reactions were first described in 1934 by L. Szilárd and T.A. Chalmers.[10] Irradiation of ethyliodide with a Ra-Be neutron source yielded traces of free iodine that could be separated from the parent compound through reduction and precipitation as silver iodide (Equation 1, page 9). A ten-fold greater specific activity of radioiodine was found in the precipitate than in the irradiated ethyl iodide.

Equation 2

$$CH_3CH_2{}^{127}I(n,\gamma)\text{“}CH_3CH_2{}^{128}I\text{”} \rightarrow CH_3CH_2{}^{\cdot} + {}^{128}I^{\cdot} \rightarrow \rightarrow Ag^{128}I\downarrow$$

Chemical (electronic) bond energies typically range from 50 kJ/mol (O_2N-N_2O) and 500 kJ/mol (O_2Cr-O) whereas the recoil energy due to the radioactive decay varies from 180-1200 GJ/mol (α emission) to > 10 GJ/mol (γ emission). Therefore, the recoil from radioactive decay can break chemical bonds of the decaying isotope.[11]

Ejected nuclei are affected by various changes: electronic configuration due to the change in atomic number and ionization/excitation. So the daughter nuclei are highly reactive and able to react in unusual ways. In liquids and solids the daughter isotope can replace the ejected target isotope, this is called retention. In solids also dislocations and defects due to localized melting may be observed.[12]

The effects of nuclear reactions on chemical compounds can be exploited to obtain high specific activity samples of radionuclides. The ejected atom may be recovered by means of chemical separation to obtain high specific and carrier-free activities.

Various chemical reactions can occur immediately after the nuclear reaction between the recoiling atom and the parent molecule: redox reactions, ligand exchange/bond breaking and bond reformation. All of these reactions are also influenced by the parent molecule. Therefore, molecules with target atoms in various stable oxidation states and little bond reformation are well suited for S-C reactions. Also, the target molecule should be thermally stable und should not decompose in radiolytic environment.

There are two main factors describing S-C reactions: enrichment factor (ratio of specific activity after separation to specific activity before separation) and by yield of the radionuclide (ratio of activity of radionuclide after separation to total activity produced – the higher the better). Often S-C reactions are also characterized by the retention (ratio of total activity produced to activity of radionuclide remaining in the target after separation -the opposite of the yield). The lower the retention, the

higher the specific activity of the isotope generated may be. A small retention also means little bond reformation. Bond reformation can be influenced by the chemical environment as substituents on the parent molecule.

The S-C reactions of chromium compounds are very well studied[13–15], whereas the chemically related molybdenum is not. In the recent years, due to the ^{99}Mo-crisis, several efforts were made to close this lack of knowledge. Among other compounds molybdenum-hexacarbonyl[16,17], molybdenumoxinate[18] and molybdenum(IV) oxophthalocyanines[19] have been studied.

The effect of neutron energy and ionizing radiation were studied in zinc, copper and cobalt phthalocyanines[20], whereas the influence of irradiation time and neutron flux were studied with molybdenum(IV) oxophthalocyanines elsewhere.[19] Substituent effects in nuclear reactions, especially in phthalocyanines have yet to be reported and may yield valuable information about the nature of chemical recombination processes following nuclear recoil.

3 Task

Substituent effects in molybdenum(IV) oxophthalocyanines (MoOPc; Pc = phthalocyanine dianion $C_{32}H_{16}N_8^{2-}$) were studied in Szilárd-Chalmers reactions, especially the influence on the recoil of ^{99}Mo. Synthesis and characterization of the target materials as well as irradiation experiments and radioanalytical measurements were carried out to quantify these effects.

As target materials molybdenum(IV) oxophthalocyanine (1) and nitro- (2), methyl- (3) and fluoro- (4) substituted molybdenum(IV) oxophthalocyanine were chosen. Molybdenum(IV) oxophthalocyanines are chemically and thermally very stable and the target molecule molybdenum is in the desired oxidation state +IV. Usually these compounds are blue/green pigments and dyes.[21]

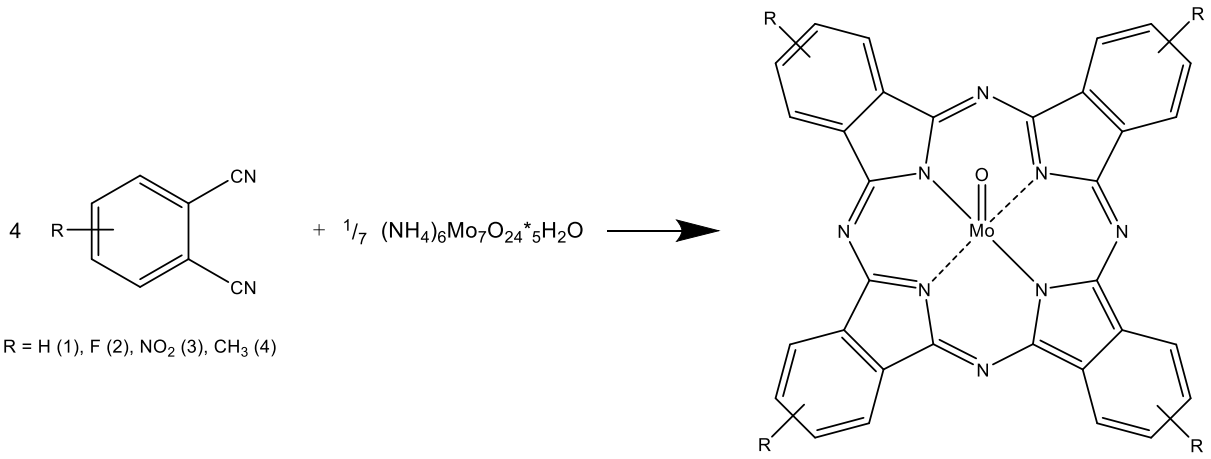

Figure 5: reaction scheme for the synthesis of substituted molybdenum(IV) oxophthalocyanines

Syntheses of the target materials are straight forward and do not require any solvent: neat 1,2-dicyanobenzenes and ammonium heptamolybdate tetrahydrate react in the melt at about 170 °C to yield the desired product (Figure 5).[22] The resultant materials may be purified by sublimation and recrystallization.

Irradiation with thermal neutrons in the TRIGA Mark II research reactor and yields and retention of ^{99}Mo will be established. The results will be examined regarding the functionality and its influence on the parameters quantified.

4 Results and Discussion

4.1 Synthesis and Purification

Successful syntheses of un-, fluoro-, nitro- and methyl-substituted molybdenum(IV) oxophthalocyanines in yields varying from 48–70 % were performed. Syntheses were performed in open, sealed and evacuated glass tubes without any significant changes in yield. During the reaction in open tubes the starting material had slightly greater tendency to evaporate. Also a slight smell of ammonia could be observed during the reaction as ammonia is both a by-product and necessary catalyst for the reaction.

Purification of the materials proved very challenging. As the solubility of the target molecules is quite low, a suitable solvent was sought (see Table 2).

Table 2: Solubility of the products

	(1) H	(2) F	(3) NO_2	(4) CH_3
Ethylacetate	-	-	-	~, green-yellow
Acetone	-	-	-	+, green
2-propanol	-	-	-	-
H_2SO_4 conc.	+, brown	+, brown; after 24 h colourless	+, brown	+, green
Toluene	-	-	-	-
Diethylether	-	-	-	-
DMSO	-, pale blue	-	-, pale yellow	~, darkgreen
Nitrobenzene	-	-	~, pale green	~, darkgreen
Nitromethane	-		-	~, darkgreen
1,2,4-trichlorobenzene	+ (Δ), green	+ (Δ), green	~ (Δ), brown	+, green

- Insoluble; ~ slightly soluble; + soluble; Δ heat

All substances, except the nitro-substituted (2), are soluble in hot 1,2,4-trichlorobenzene. Recrystallization from this solvent was not satisfactory, as large amounts of solvent were necessary to dissolve macroscopic amounts of the material. Sulfuric acid is described as suitable solvent in several publications[23,24], but was not used here as the dissolution process seemed to destroy the materials under study. Subliming in high vacuum at 0.06 mbar and 450 °C was apparently successful for (1) and (3).

4.2 Characterization

4.2.1 Thermal analysis

Thermal analysis was used to gain insight into the syntheses of the phthalocyanines: potential loss of substrates, possible impurities and temperature profile of the melt reaction itself.

Due to the high thermal stability of the products, measurement of melting point (zone) was not trivial. In (1), (2) and (4) some colourless impurities started melting at 250 °C, however, no other visible transformation was observed. In (3) melting of green crystals were observed at 210 °C.

Regarding DSC and TGA measurements, reaction is initiated from 200-235 °C, depending of the reaction mixture (see Table 4, page 27). Measurements of the products show very good thermal stability and nearly no decomposition which fits well with the difficulty in determining melting points and is highly desirable for target materials subjected to a radiolytic environment.

4.2.2 Spectral analysis

4.2.2.1 IR Spectra

Comparison of the calculated (994 cm^{-1}, unscaled) and measured (965 cm^{-1}) Mo=O vibration for molybdenum(IV) oxophthalocyanine shows a good correlation. Also theoretical calculation of the Mo≡N (1078 cm^{-1}) vibration was done but was not detected in any measured IR spectra. A Mo≡N vibration would have indicated an oxidation state +V, the Mo=O vibration indicates the desired oxidation state +IV. Also the reported values for the Mo=O vibration are agree very well[23–25].

In (2), (3) and (4) typically IR bands indicative of the desired substituent could be observed: C-F stretching vibrations (1327 cm^{-1}), NO_2 stretching vibration (1422 and 1336 cm^{-1}) and the C-H stretching vibration (2920 cm^{-1}).

4.2.2.2 UV/VIS Spectra

As the UV/VIS spectra were not measured in solution, comparison of the results with known data is very difficult. In all measured spectra a very broad peak from 600-900 cm^{-1} could be observed. More details were not apparent due to poor resolution.

4.2.2.3 Powder X-ray diffraction

In all measured diffractograms diffraction lines at the following values of 2θ° were observed: 92.50, 110.00, 115.23. In the spectra of (1) and (4) a very strong line at 7.73 and a strong line at 13.64 appeared. The pattern of (2) and (3) gave fewer lines than (1) and (4). The powder X-ray diffraction pattern which we calculated from the X-ray crystallographic data[25] was different from ours, which may be explained by a different crystal modification as polymorphism is not uncommon in metal-phthalocyanines [26,27].

4.3 Irradiation Experiments

Irradiation experiments were successful for all compounds synthesized and led to the expected yields (see Figure 6). Highest yields were obtained with (1) and (3), about 25 % less with (2) and (4).

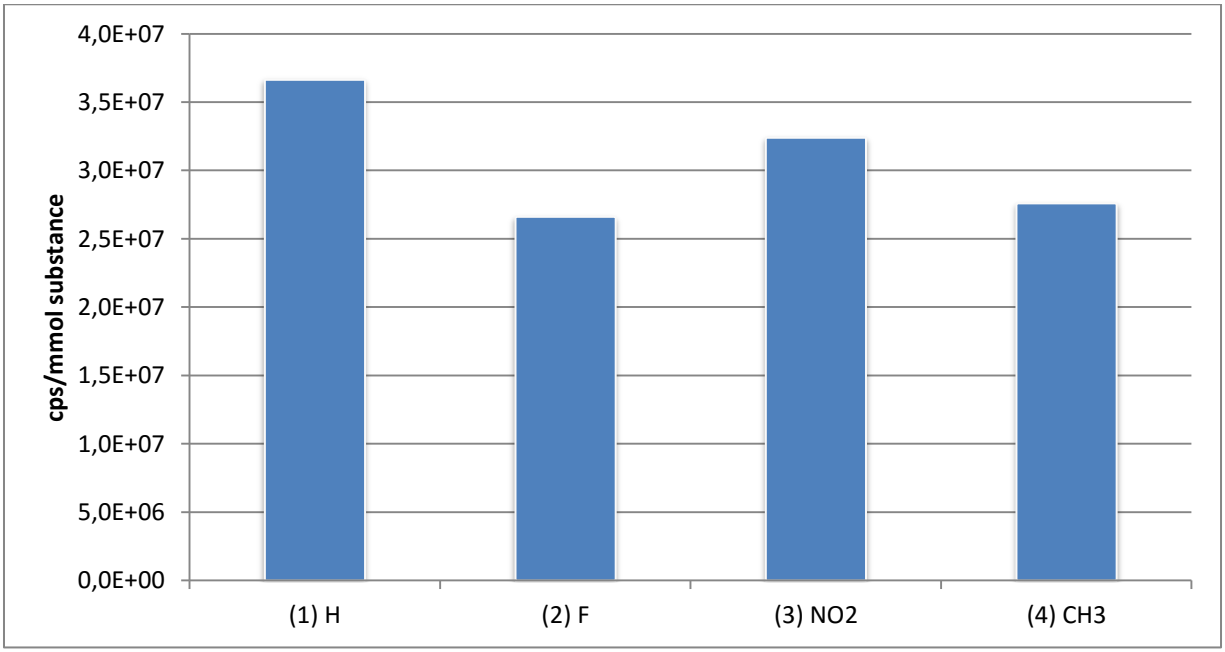

Figure 6: radiochemical yields after irradation, before separation

An explanation could be the influence of the substituent or differences in the purity of the substances irradiated since purification of the target materials was challenging.

The ^{99}Mo retention upon irradiation (see Figure 7) was found to be very promising for (4) with retention of only 3.3 %, (1) and (2) show moderate retention with 13.5 % and 10.0 %, respectively and only (2) shows an excessive retention of ^{99}Mo in the target material with almost 30 % activity retained. The high retention of (2) may be explained by the reactivity of the fluoro substituent which can lead to more recombination reactions and, therefore, to a higher perceived retention. (2) should also be discussed separately, as it gave the lowest radiochemical yield. Compared to the other substances (2) has the lowest solubility, but purification by sublimation was successful. The low yield may be an indicator of lower purities as the yield is determined by the amount of molybdenum.

The low retention and good yield, as well as the relatively easy purification of (4) make it a good starting point for further investigations.

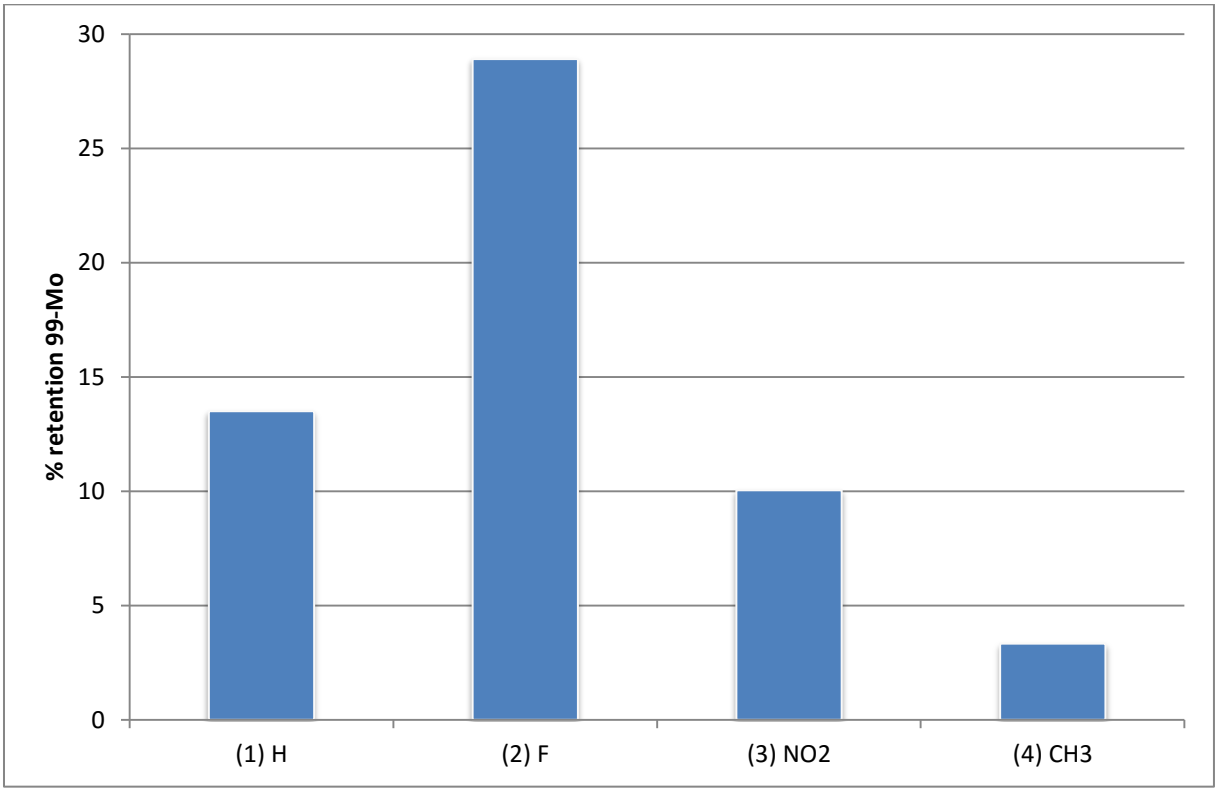

Figure 7: Retention of ^{99}Mo – percentage of the activity of ^{99}Mo remaining in the target

4.3.1 Substituent effects[28,29]

As the retention depends, among other factors, on recombination processes between the ejected activated nuclei and the target, a deeper understanding of these reactions will be useful for the design of future targets. Different substituents have different electronegativities and other electronic properties which may influence the chemistry of the active site of the molecule depending on the distance between the substituent and that site. To eliminate steric effects, only substituents in meta or para positions of the aromatic system are used. As the substituents seem to have an impact, their influence may be examined in more detail using Linear Free Energy Relationships (LFER). LFER is the relation between the logarithms of equilibrium constants *K* or rate constants *k*. It is an indirect method and especially useful for reactions that cannot be examined in other ways. Therefore, Hammett-plots were used to examine the electronic effects substituents may cause in recombination reactions.

The Hammett parameter σ_X is defined as the logarithm of the ratio of the acidity constant of benzoic acid derivatives $k_a(X)$ and unsubstituted benzoic acid $k_a(H)$ (Equation 3).

Equation 3

$$\log\left(\frac{k_a(\mathrm{X})}{k_a(\mathrm{H})}\right) = \sigma_\mathrm{X}$$

Reactions are related to this reference reaction using the Hammett-equation (Equation 4).

Equation 4

$$\log\left(\frac{K_\mathrm{X}}{K_\mathrm{H}}\right) = \rho\sigma_\mathrm{X}$$

Plotting the Hammett parameter σ_X against $log(K_X/K_H)$ in which K_X is the equilibrium constant (or indicator thereof) for the reaction under study with the substituted substrate and K_H that for the reaction of the unsubstituted substrate (or indicator thereof) gives the sensitivity constant ρ as slope. Instead of using equilibrium or rate constants many measurable parameters may be used to examine a particular reaction.

The sensitivity constant ρ gives information about the sensitivity to substituent effects of the reaction compared to benzoic acid, as well as the charge involved in the rate-determining step of the reaction:

- $\rho > 1$ reaction more sensitive to substituents, negative charge
- $1 > \rho > 0$ reaction less sensitive to substituents, negative charge
- $0 \sim \rho$ no substituent effect, no change in charge
- $\rho < 0$ positive charge

The magnitude of ρ is an indicator of the sensitivity of the reaction to electronic effects. It also may be an indicator of multiple reaction pathways.

Non-linearity of the slope does not automatically preclude substituent effects. If it is possible to lay two lines with different slopes, there may be a change in the mechanism depending on the substituent. It is also possible that two different mechanisms are acting, depending on the substituent position meta or para. Also, bending in a Hammett-plot contains information: an increase in slope indicates a change in the mechanism. A decrease in slope is indicative of the same mechanism, but a change in the rate-determining step.

To obtain some insight into the influence of the substituents and the nature of recombination reactions, a Hammett-plot was generated plotting yield and retention against sigma (Figure 8). The points using the "yield" appear in a nearly straight line with slope 0. Regarding the information that can be extrapolated from ρ, the yield is not affected from substituent effects. This is expected, as the yield depends only on the physical parameters during irradiation as the neutron flux. Also no change in charge should be involved regarding the yield, which also fits well.

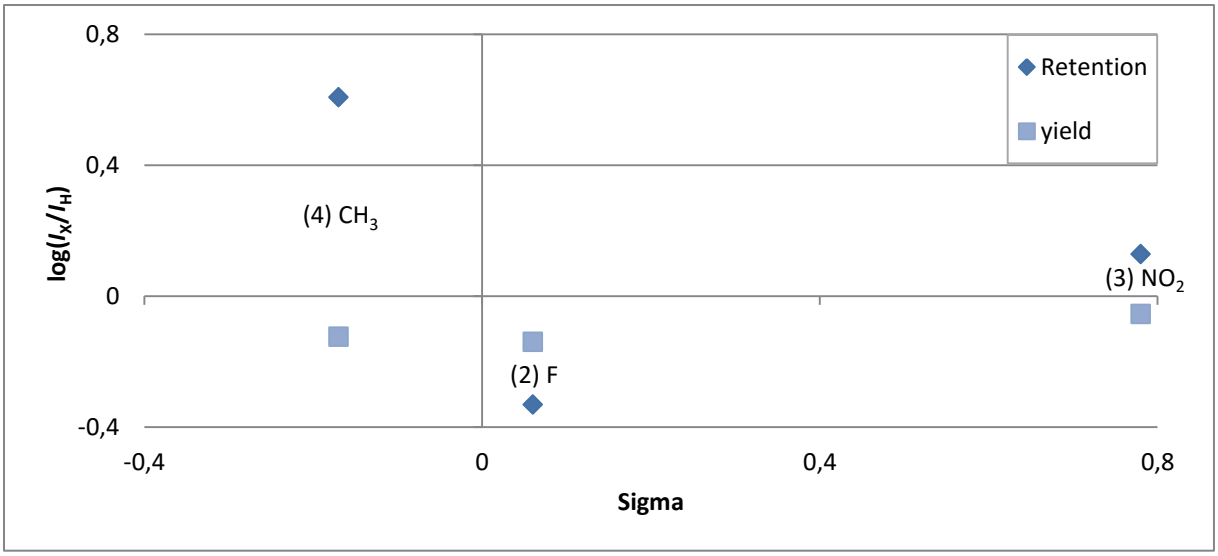

Figure 8: Hammett plot for yield and retention using the intensity I (see 5.4.3, page 28)

At the first glance the Hammett-plot using the retention does not show any trends. But if the second point (F-substituted) may be considered as outlier, there could be a trend observed (Figure 9). The F-substituted may be considered as outlier, as the radiochemical yield as well the retention differs significantly from the other compounds.

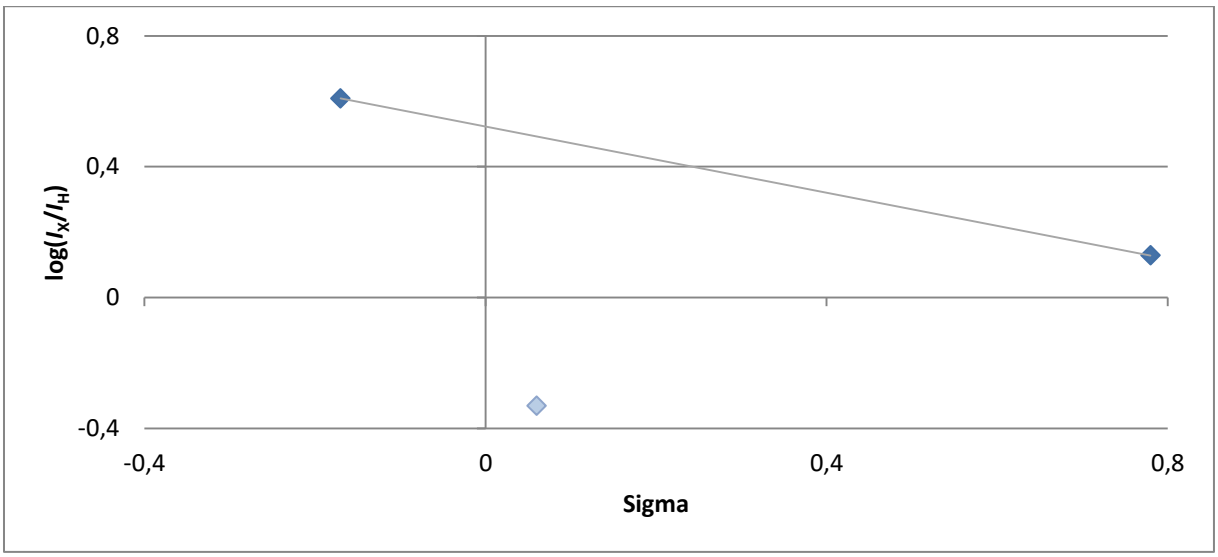

Figure 9: Hammett-plot for retention using the intensity I (see 5.4.3, page 28), with (2) F as outlier

The negative suggests that a positive charge involved in the recombination reaction. This seems reasonable as the reaction should involve highly ionized species. Similarly electrophilic aromatic reactions display a negative slope, so a similar mechanism involving a cationic rate determining transition state might be postulated. The slope observed in the Hammett-plot might also be considered unexpected since recombination reactions have been suggested to occur at epithermal energies and should, therefore, be only minimally effected by the chemistry (the electronic environment) of the target substance.[11]

5 Experimental part

5.1 General

If not described otherwise, the following chemicals were used without further purification.

Ammonium heptamolybdate tetrahydrate, crystalline - österreichische Heilmittelstelle
1,2-Dicyanobenzene, 98 % - Aldrich chemistry
1,2-Dicyano-4-fluorobenzene, ≥ 99.0 % - Aldrich chemistry
1,2-Dicyano-4-nitrobenzene, 97 % - Alfa Aesar
1,2-Dicyano-4-methylbenzene, 99 % - Aldrich chemistry
Dichloromethane, > 99.5 %, for synthesis – Roth
Ammonia-solution, 25 %, p.a. – Riedel-de-Haën

Mid range infrared spectra were recorded by the ATR technique within the range of 4000-450 cm^{-1} using a Perkin Elmer Spectrum Two FTIR spectrometer with an UATR accessory attached. If not otherwise stated, the background was measured with the anvil open to ambient air.

Solid state UV/Vis NIR spectra were recorded on a Perkin Elmer Lambda 900 spectrophotometer between 320 and 1200 nm in diffuse reflectance against $BaSO_4$ as background. A powder sample holder in "Praying Mantis" configuration was used.

Theoretical calculations were generated using Gaussian 09 Rev.D01[30] implemented on the Vienna Scientific Cluster 3 (VSC-3)and visualized using GaussView 5.0.8. The calculations were run using density functional theory with the hybrid functional B3LYP [31–33] using the SDD basis set. Output files are available on request.

Powder X-ray diffraction measurements were carried out on a PANalytical X'Pert diffractometer in Bragg Brentano geometry using Cu-K$\alpha_{1,2}$ radiation, an X'Celerator linear detector with a Ni filter, sample spinning with back loading zero background sample holders and 2θ = 4-120 ° T = 24 C at the X-ray Center of the Vienna University of Technology in collaboration with Werner Artner. The diffractograms were evaluated using the PANalytical program suite HighScorePlus v3.0d. A background correction and a $K_{\alpha 2}$ strip were performed.

TGA/DSC (TGA: thermogravimetric analysis, DSC: differential scanning calorimetry) analyses were carried out on a Netzsch STA 449 F1 Jupiter system with a heating rate of 10 K/min under N_2 atmosphere in crimp-sealed Al crucibles with a pinhole in the lid was used between 20 °C and 400 °C. The measurements were corrected against an empty crucible.

Irradiation was carried out in dry irradiation tubes at the edge of a TRIGA Mark II reactor with a power of 250 kW and a neutron flux of $2 \cdot 10^{12}$ $cm^{-2}s^{-1}$.

Gamma-spectrometry was performed with a 151 cm^3 HPGe-detector from Canberra Industries (1.8 keV resolution at the 1332 keV ^{60}Co peak; 50.1 % relative efficiency), connected to a PC-based multi-channel analyzer with preloaded filter and Loss-Free Counting (LFC) system.

5.2 Synthesis of the molybdenum(IV) oxophthalocyanines

5.2.1 (1) unsubstituted

1,2-Dicyanobenzene (865 mg, 6.75 mmol) and ammonium heptamolybdate tetrahydrate (212 mg, 0.172 mmol) were ground together and sealed in a glass tube (15 cm length, 1.3 cm diameter). The reaction mixture was heated to ~170 °C in a sand bath overnight. After cooling to room temperature the sealed glass tube was opened and the black residue soaked in dichloromethane (50 mL) over 72 h. After washing the entire solid product out of the glass tube with dichloromethane the solution and the black residue were then centrifuged (3 min, 3000 rpm, 3 times) and the supernatant carefully removed. Drying the residue overnight in air yielded 366 mg (48.8 %) of dark blue powder. Sublimation at 450 °C and 0.06 mbar gave a dark blue powder which appeared black turquoise because of prior sublimation of starting material.

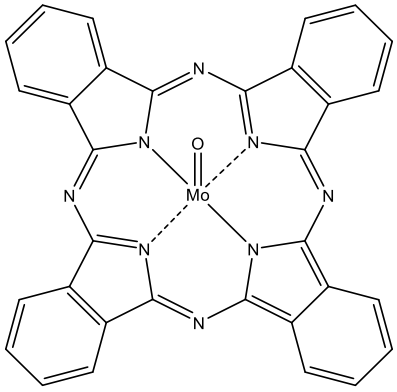

$C_{32}H_{16}MoN_8O$

624.5 g/mol

m.p. [°C]: > 300

IR [cm^{-1}]: 2924, 1607, 1493, 1475, 1413, 1330, 1286, 1158, 1116, 1085, 1062, 965 (Mo=O), 895, 876, 837, 775, 752, 722, 638, 569, 504

Powder X ray diffraction 2θ° [Å]: 7.73, 10.68, 12.95, 13.64, 16.59, 17.27, 18.64, 22.73, 25.23, 25.91, 29.09, 92.50, 110.00, 115.23

5.2.2 (2) Fluoro substituted

1,2-Dicyano-4-fluorobenzene (906 mg, 6.20 mmol) and ammonium heptamolybdate tetrahydrate (219 mg, 0.178 mmol) were ground together and fused in a glass tube. The reaction mixture was heated to ~170 °C in a sand bath overnight. After cooling to room temperature the sealed glass tube was opened and the black residue soaked in dichloromethane (50 mL) over 72 h. The solution and the black residue were then centrifuged (3 min, 3000 rpm, 3 times) and the supernatant carefully removed. Drying the residue overnight yielded 520 mg (69.4 %) of dark blue powder. Sublimation at 400 °C and 0.20 mbar gave a dark green powder.

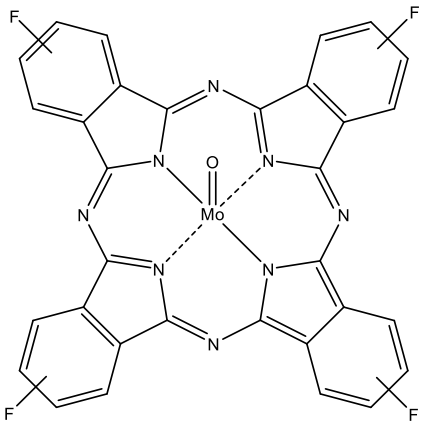

$C_{32}F_4H_{12}MoN_8O$

696.5 g/mol

m.p. [°C]: > 300

IR [cm^{-1}]: 2920, 1609, 1477, 1396, 1327, 1256, 1220, 1109, 1082, 1045, 971 (Mo=O), 944, 868, 820, 770, 751, 725, 639, 511, 490

Powder X ray diffraction 2θ° [Å]: 26.82, 28.18, 92.73, 110.00, 115.23

5.2.3 (3) Nitro substituted

1,2-Dicyano-4-nitrobenzene (1093 mg, 6.31 mmol) and ammonium heptamolybdate tetrahydrate (214 mg, 0,173 mmol) were ground together and fused in a glass tube. The reaction mixture was heated to ~170 °C in a sand bath overnight. After cooling to room temperature the sealed glass tube was opened and the black residue soaked in dichloromethane (50 mL) over 72 h. The solution and the black residue were then centrifuged (3 min, 3000 rpm, 3 times) and the supernatant carefully removed. Drying the residue overnight yielded 499 mg (66.6 %) of dark green powder. Sublimation at 410 °C and 0.07 mbar was not successful, as the product turned black subsequently to carbonization.

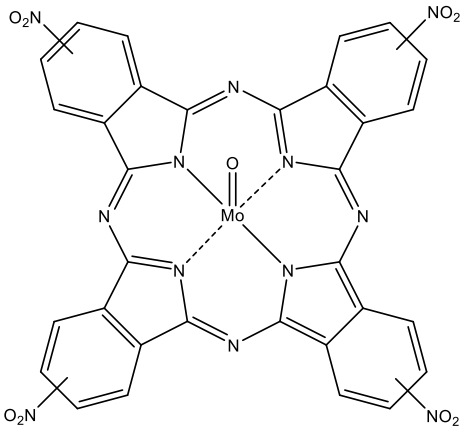

$C_{32}H_{12}MoN_{12}O9$

804.5 g/mol

m.p. [°C]: > 300

IR [cm^{-1}]: 3089, 1737, 1610, 1522 (NO_2), 1336 (NO_2), 1254, 1135, 1087, 1005, 978 (Mo=O), 915, 839, 808, 758, 732, 680, 661, 476

Powder X ray diffraction 2θ° [Å]: 24.09, 26.14, 27.95, 34.32, 50.00, 92.50, 110.00, 115.23

5.2.4 (4) Methyl substituted

1,2-Dicyano-methylbenzene (955 mg, 6.72 mmol) and ammonium heptamolybdate tetrahydrate (217 mg, 0,175 mmol) were ground together and fused in a glass tube. The reaction mixture was heated to ~170 °C in a sand bath overnight. After cooling to room temperature the sealed glass tube was opened and the black residue soaked in dichloromethane (50 mL) over 72 h. The solution and the black residue were then centrifuged (3 min, 3000 rpm, 3 times) and the supernatant carefully removed. Drying the residue overnight yielded 411 mg (54.9 %) of dark green powder. Sublimation at 450 °C and 0.06 mbar gave a dark blue powder which appeared turquoise-black because of prior sublimation of starting material.

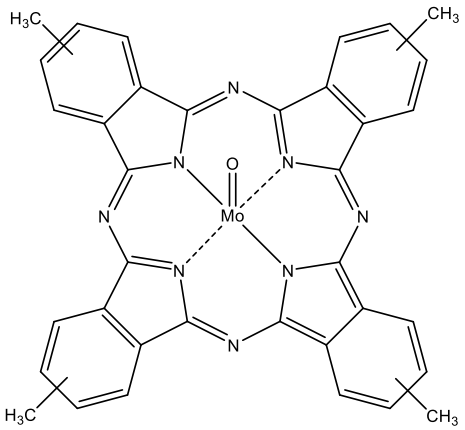

$C_{36}H_{24}MoN_8O$

680.5 g/mol

m.p. [°C]: 210

IR [cm^{-1}]: 2920 (C-H), 2232, 1719, 1601, 1572, 1519, 1353 (C-CH3), 1097, 1014, 891, 821, 741, 627, 563, 527

Powder X ray diffraction 2θ° [Å]: 7.73, 11.59, 11.82, 13.64, 15.23, 17.05, 26.36, 27.50, 88.64, 92.50, 110.00, 112.50, 115.00

5.3 Characterization

5.3.1 Differential scanning calorimetry (DSC) and thermogravimetric analysis (TGA)

All measurements were obtained with a heating rate from of 10 C/min to 400 °C, holding 400 °C for 10 min and fast cooling to room temperature. Sample sizes were ~ 5 mg.

Onsets were determined as shown in Figure 10.

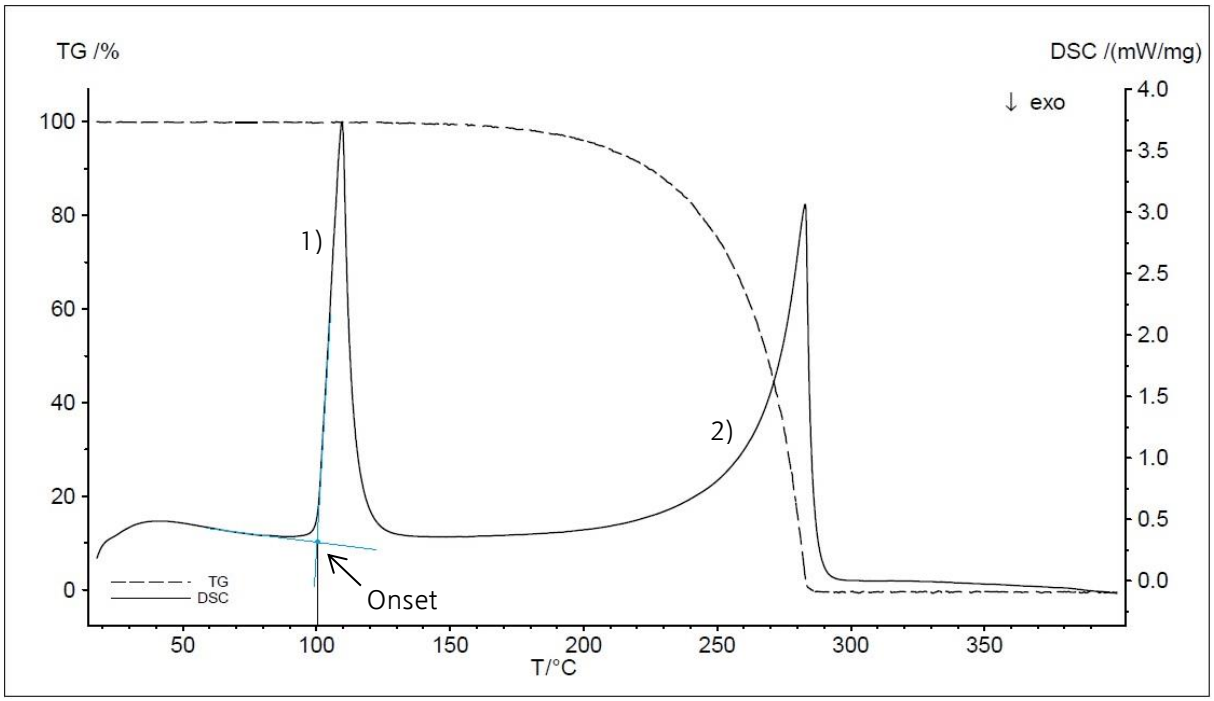

Figure 10: A representative plot for DSC and TGA of starting materials (1,2-dicyano-4-fluorobenzene) showing 1) melting and 2) evaporation

The first sharp peak in the DSC curves marks the melting of the starting material, the second the evaporation. The evaporation can also be seen in the TGA curve as weight loss.

5.3.1.1 Starting materials

As not all starting materials are >99 % pure and the impurities can influence the synthesis, all starting materials were measured by DSC and TGA.

Table 3: Onset starting materials compared to melting points from manufacturer's data

Starting Material	Onset melting[°C]	m.p. [°C] [Δ]	Onset evaporation [°C]
1,2-Dicyanobenzene	138	137-139	205[+]
1,2-Dicyano-4-fluorobenzene	99	100-104	267
1,2-Dicyano-4-nitrobenzene	131; 141	136-137	339
1,2-Dicyano-4-methylbenzene	119	119-121	270
Ammonium heptamolybdate	102	~90[◊]	-

[Δ] *manufacturer's data*
▪ *Double peak caused by impurity*
[+] *no evaporation, instead a reaction occurs, maybe polymerisation*
[◊] *decomposition*

5.3.1.2 Reaction mixtures

To determine the starting temperature of the reaction, a small aliquot of the reaction mixture was measured. Onset of the reaction mixture was determined as shown in Figure 11.

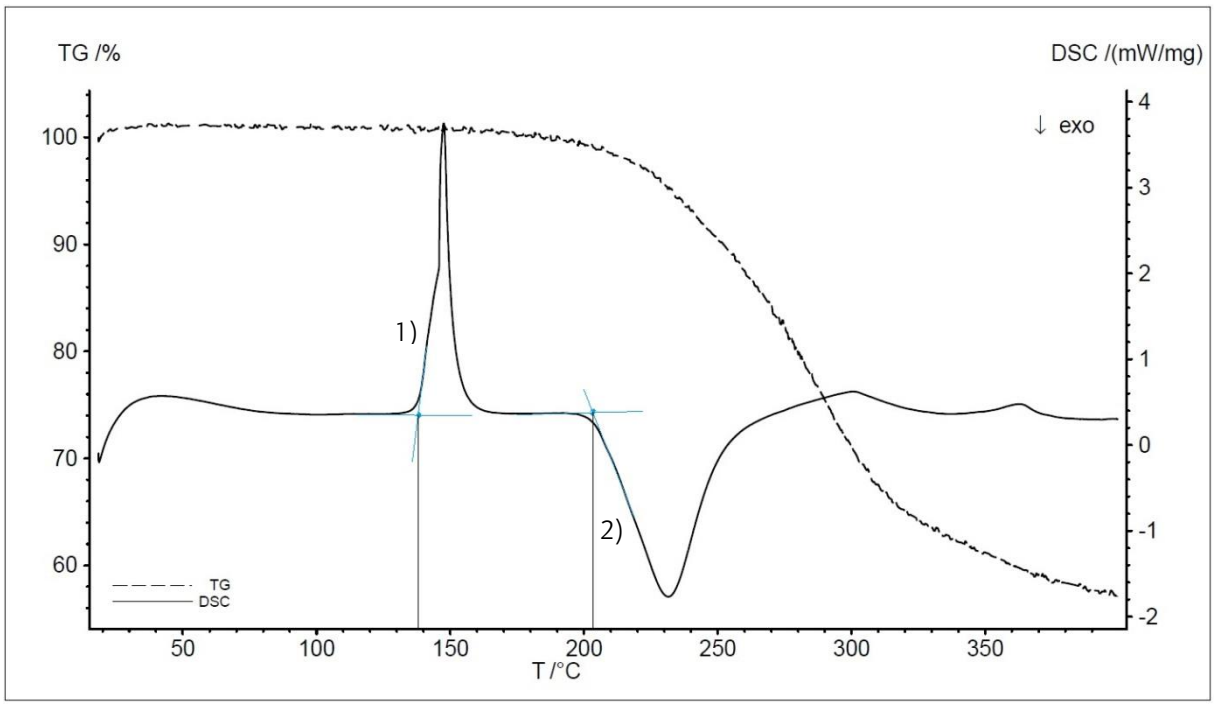

Figure 11: A representative plot for DSC and TGA of the reaction mixture for (1) showing 1) melting and 2) reaction progress

As seen in Table 4 the reaction temperature depends on the substituent of the phthalocyanines as well on the melting point of the starting material.

Table 4: Reaction onset temperatures

Reaction	Onset reaction [°C]
1,2-Dicyanobenzene	204
1,2-Dicyano-4-fluorobenzene	217
1,2-Dicyano-4-nitrobenzene	219
1,2-Dicyano-4-methylbenzene	233

5.3.1.3 Products

As the thermal stability of the products is important for the irradiation experiments it was determined by DSC and TGA.

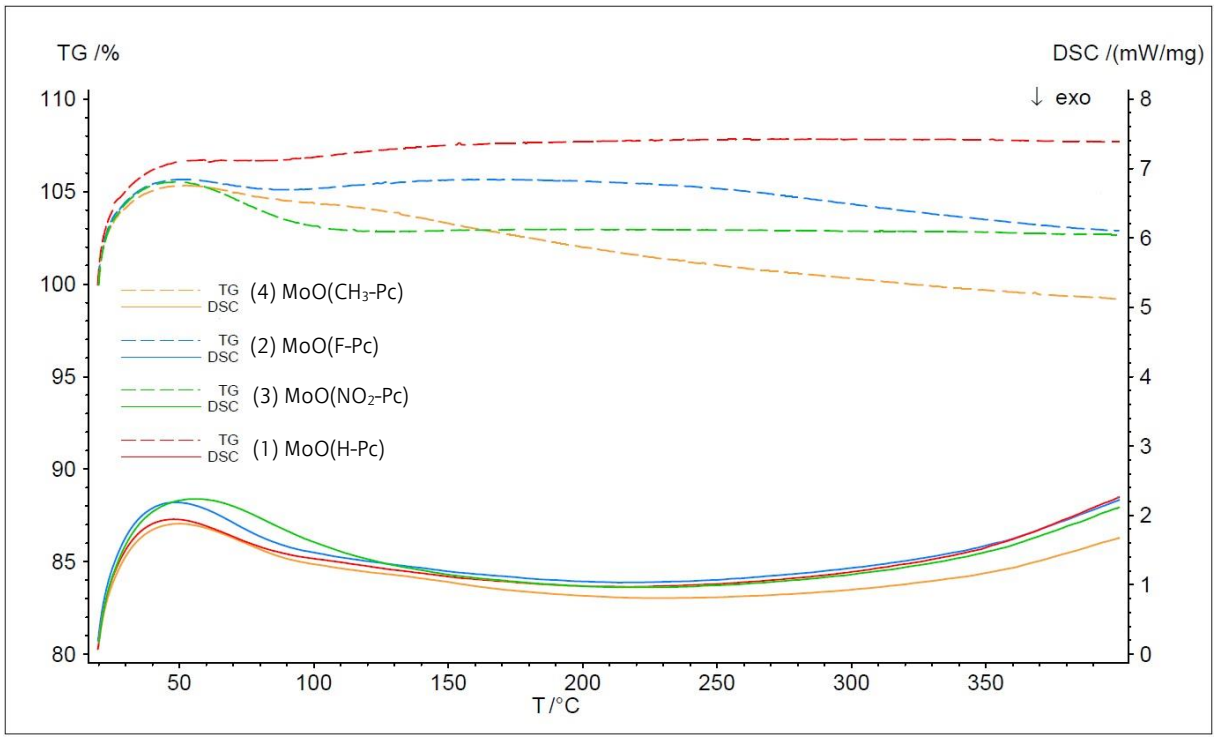

Figure 12: DSC and TGA plots for the synthesised molybdenum(IV) oxophthalocyanines (1) – (4)

In Figure 12 the TGA and DSC curves show little change over time. This indicates a high thermal stability up to 400 °C for all products.

5.4 Irradiation experiments

5.4.1 Irradiation

For neutron irradiation in the TRIGA reactor, 35–45 mg (0.06 mmol Mo) of each phthalocyanine complex were weighed into a small tube, bundled together in an irradiation capsule and irradiated for 1 h at 250 kW with a neutron flux of $2 \cdot 10^{12}$ $cm^{-2}s^{-1}$. After 20 h decay time the dose at 30 cm was 1.5 µSv/h.

5.4.2 Work-up

The irradiated samples were each suspended in 4 mL ammonia (25 %), filtered over cotton wool and rinsed with 1 mL ammonia into a closed vessel. The cotton wool and the solid residue were put in a closed vessel with 5 mL ammonia to obtain the same geometry for the gamma spectroscopy.

5.4.3 Gamma spectroscopy

Gamma spectra were recorded for 300 s directly after the work-up and 72 h afterwards. For the calculation of the retention, the peak maximum *I* at 181 keV from ^{99}Mo was decay-corrected to the end of the irradiation. To correct for the variation in sample mass, the activities were normalized to 1 mmol of substance.

6 Conclusion

Syntheses of substituted (-H, -F, -NO_2, -CH_3) molybdenum(IV) oxophthalocyanines were successful. Due to difficulties in purification the characterization was challenging. Successful irradiation of the compounds synthesized was performed. Calculation of the retention shows the influence of the substituents on recombination reactions. Investigation thereof with Linear Free Energy Relationships (Hammett-equation) suggests a positive charge is involved in the rate-determining recombination step. As similar electrophilic reactions also display a negative slope, an analogous mechanism might be postulated. Since recombination reactions have been suggested to occur at epithermal energies and should, therefore, be only minimally effected by the chemistry of the target substance, this observation may be considered unexpected. More experiments and data are needed to make a definitive statement.

7 References

(1) Kónya, J.; Nagy, N. M. *Nuclear and Radiochemistry*; Elsevier Inc., 2012.

(2) Choppin, G.; Liljenzin, J.-O.; Rydberg, J.; Ekberg, C. *Radiochemistry and Nuclear Chemistry*, 4th ed.; Elsevier, 2013.

(3) Committee on Medical Isotope Production Without Highly Enriched Uranium; Council, N. R. *Medical Isotope Production Without Highly Enriched Uranium*; National Academies Press: Washington, D.C., 2009.

(4) Glaser, A. On the Proliferation Potential of Uranium Fuel for Research Reactors at Various Enrichment Levels. *Science and global Security* **2006**, *14* (1), 1–24. DOI: 10.1080/08929880600620542.

(5) Vandegrift, G. F. Facts and Myths Concerning ^{99}Mo Production with HEU and LEU Targets. *2005 International RERTR Meeting*; 2005.

(6) Steinhauser, G.; Lechermann, M.; Axelsson, A.; Böck, H.; Ringbom, A.; Saey, P. R. J.; Schlosser, C.; Villa, M. Research Reactors as Sources of Atmospheric Radioxenon. *J. Radioanal. Nucl. Chem.* **2013**, *296* (1), 169–174. DOI: 10.1007/s10967-012-1949-x.

(7) Kolar, Z. I.; Okx, W. J. C.; Kloosterman, J. L. *Assessment of Molybdenum-99 Production from High-Enriched Uranium (HEU) Targets in Comparison with That from Low-Enriched Uranium (LEU) Targets*; 2002.

(8) Nuclear Energy Agency. *The Supply of Medical Radioisotopes Review of Potential Molybdenum-99/Technetium-99m Production Technologies*; 2010.

(9) Oganessian, Y. T.; Dmitriev, S. N.; Kliman, J.; Maslov, O. A.; Starodub, G. Y.; Belov, A. G.; Tretiakova, S. P. RIB Production with Photofission of Uranium. *Nucl. Phys. A* **2002**, *701*, 87–95. DOI: 10.1016/S0375-9474(01)01553-6.

(10) Szilard, L.; Chalmers, T. A. Chemical Separation of the Radioactive Element from Its Bombarded Isotope in the Fermi Effect. *Nature* **1934**, *134* (3386), 462–462. DOI: 10.1038/134462b0.

(11) Kratz, J.-V.; Lieser, K. H. *Nuclear and Radiochemistry Fundamentals and Applications Volume 2*, 3rd, revis ed.; Wiley-VCH Verlag GmbH & Co. KGaA, 2013.

(12) Müller, H. Hot Atom Chemistry in Inorganic Solids — The Present Status and Future Aspects. *Radiochim. Acta* **1981**, *28* (4), 233–239. DOI: 10.1524/ract.1981.28.4.233.

(13) Harbottle, G. Szilard-Chalmers Reaction in Crystalline Compounds of Chromium. *J. Chem. Phys.* **1954**, *22* (6), 1083. DOI: 10.1063/1.1740269.

(14) Harbottle, G.; Maddock, A. G. The Preparation of Chromium–51 of High Specific Activity. *J. Chem. Phys.* **1953**, *21* (10), 1953. DOI: 10.1063/1.1698643.

(15) Fishman, L. M.; Harbottle, G. The Szilard-Chalmers Reaction in Aqueous Solutions of Tri- and Hexavalent Chromium. *J. Chem. Phys.* **1954**, *22* (6), 1088–1093. DOI: 10.1063/1.1740270.

(16) Colonomos, M.; Parker, W. Preparation of Carrier-Free ^{99}Mo by Means of (n,γ) Recoil. *Radiochim. Acta* **1969**, *12* (3), 163–164. DOI: 10.1524/ract.1969.12.3.163.

(17) Krüger, A.; Lieser, K. H. On the Preparation of ^{99}Mo of High Specific Activity by Szilard-Chalmers Reactions. *Radiochim. Acta* **1981**, *28* (1), 29–34. DOI: 10.1524/ract.1981.28.1.29.

(18) Tomar, B. S.; Steinebach, O. M.; Terpstra, B. E.; Bode, P.; Wolterbeek, H. T. Studies on Production of High Specific Activity ^{99}Mo and ^{90}Y by Szilard Chalmers Reaction. *Radiochim. Acta* **2010**, *98* (8), 499–506. DOI: 10.1524/ract.2010.1744.

(19) Baba, S.; Moki, T. Preparation of ^{99}Mo by the Use of the Szilard-Chalmers Effect with Oxymolybdenum Phthalocyanine. *Radiochim. Acta* **1981**, *29* (2–3), 135–137.

(20) Apers, D. J.; Dejehet, F. G.; van Outryve d'Ydewalle, B. S.; Capron, P. C. Chemical Effects of Nuclear Recoil: Metal Phthalocyanines. *J. Inorg. Nucl. Chem.* **1962**, *24* (7), 927–930. DOI: 10.1016/0022-1902(62)80117-1.

(21) McKeown, N. B. Product Class 9: Phthalocyanines and Related Compounds. In *Science of Synthesis - Volume 17*; Thieme, 2004; p 1237ff.

(22) Gorsch, M.; Homborg, H. Ein- Und Zweikernige MoII-Phthalocyaninate(2-): Darstellung Und Eigenschaften von Bis(cyano)phthalocyaninato(2-)molybdat(II) Und Bis(phthalocyaninato-(2-)molybdän(II)). *Z. Anorg. Allg. Chem.* **1998**, *624* (4), 634–641.

(23) Edmondson, S. J.; Mitchell, P. C. H. Molybdenum Phthalocyanine. *Polyhedron* **1986**, *5* (1–2), 315–317. DOI: 10.1016/S0277-5387(00)84928-1.

(24) Hill, H. A. O.; Norgett (née Wansey), M. M. A Molybdenum Phthalocyanine. *J. Chem. Soc. A Inorganic, Phys. Theor.* **1966**, No. 10, 1476–1478. DOI: 10.1039/j19660001476.

(25) Boerschel, Volker; Straehle, J. Synthese Und Struktur von Oxo-Phthalocyaninato-molybdän(IV). *Zeitschrift fuer Naturforschung, Tl. B Anorg. Chemie, Org. Chemie* **1984**, *39B* (12), 1664–1667.

(26) Bernstein, J. *Polymorphism in Molecular Crystals*; Oxford University Press, 2002.

(27) Law, K.-Y. Organic Photoconductive Materials: Recent Trends and Developments. *Chem. Rev.* **1993**, *93*, 449–486. DOI: 10.1021/cr00017a020.

(28) Anslyn, E. V; Dougherty, D. A. *Modern Physical Organic Chemistry*; University Science Books, 2006.

(29) Chapman, N. B.; Shorter, J. *Advances in Linear Free Energy Relationships*; Plenum Press, 1972.

(30) Frisch, M. J. Gaussian 09. *Gaussian Inc.* Gaussian Inc.: Wallingford, CT, USA 2009.

(31) Lee, C. T.; Yang, W. T.; Parr, R. G. Development of the Colle-Salvetti Correlation-Energy Formula into a Functional of Electron-Density. *Physcial Rev. B* **1988**, *37* (2), 785–789.

(32) Becke, A. D. Density-Functional Thermochemistry. 3. The Role of Exact Exchange. *J. Chem. Phys.* **1993**, *98* (7), 5648–5652.

(33) Stephens, P. J. Ab-Initio Calculation of Vibrational Absorption and Circular-Dichroism Spectra Using Density-Functional Forve-Fields. *J. Phys. Chem.* **1994**, *98* (45), 11623–11627.